Electronic Supplementary Material (ESI) for RSC Advances.

Electronic Supplementary Information

Synthesis and photophysical properties of phenanthroimidazole-triarylborane dyads: Intriguing 'turn-on' sensing mediated by fluoride anion

Dong Kyun You,[a] Seon Hee Lee,[b] Ji Hye Lee,[a] Sang Woo Kwak,[c] Hyonseok Hwang,[a] Junseong Lee,[d] Yongseog Chung,*[c] Myung Hwan Park*[b] and Kang Mun Lee*[a]

[a] Department of Chemistry and Institute for Molecular Science and Fusion Technology, Kangwon National University, Chuncheon, Gangwon 24341, Republic of Korea

[b] Department of Chemistry Education, Chungbuk National University, Cheongju, Chungbuk 28644, Republic of Korea

[c] Department of Chemistry, Chungbuk National University, Cheongju, Chungbuk 28644, Republic of Korea

[d] Department of Chemistry, Chonnam National University, Gwangju 61186, Republic of Korea.

Table S1. Crystallographic data and parameters for **1Ph** and **1BP**

Compound	**1Ph**	**1BP**·$(THF)_{0.5}$
Formula	$C_{45}H_{39}BN_2$	$C_{107}H_{96}B_2N_4O$
Formula weight	618.59	1475.49
Crystal system	triclinic	monoclinic
Space group	P_{-1}	$P2_1/n$
a (Å)	8.6872(2)	10.8270(2)
b (Å)	13.4379(3)	11.8600(2)
c (Å)	17.4444(4)	34.3648(7)
α (°)	84.593(2)	90
β (°)	83.569(2)	94.6387(13)
γ (°)	84.507(2)	90
V (Å^3)	2007.12(8)	4398.27(14)
Z	2	2
ρ_{calc}(g cm^{-3})	1.024	1.114
μ (mm^{-1})	0.059	0.064
F(000)	656	1568
T (K)	296(2)	273(2)
Scan mode	*multi-scan*	*multi-scan*
hkl range	−10 → +10, −13 → +16, −20 → +20	−12 → +13, −14 → +12, −41 → +41
Measd reflns	26782	56695
Unique reflns [R_{int}]	7323 [0.0272]	8079 [0.0673]
Reflns used for refinement	7323	8079
Refined parameters	3913	3632
R_1[a] (I > 2σ(I))	0.0561	0.0769
wR_2[b] all data	0.1469	0.2688
GOF on F^2	1.009	1.044
ρ_{fin} (max/min) (e Å^{-3})	0.197, −0.237	0.581, −0.214

[a] $R_1 = \sum||Fo| - |Fc||/\sum|Fo|$. [b] $wR_2 = \{[\sum w(Fo2 - Fc2)2]/[\sum w(Fo2)2]\}^{1/2}$.

Table S2. Selected bond lengths (Å) and angles (deg) for **1Ph** and **1BP**

Compound	**1Ph**	**1BP**
	Bond lengths	
B(1)–C(1)	1.570(3)	1.574(6)
B(1)–C(10)	1.569(3)	1.582(6)
B(1)–C(19)	1.557(3)	1.555(5)
N(1)–C(22)	1.444(2)	–
N(1)–C(28)	–	1.450(5)
	Angles	
C(1)–B(1)–C(10)	121.37(18)	121.9(3)
C(1)–B(1)–C(19)	118.2(2)	120.4(4)
C(10)–B(1)–C(19)	120.39(19)	117.6(3)

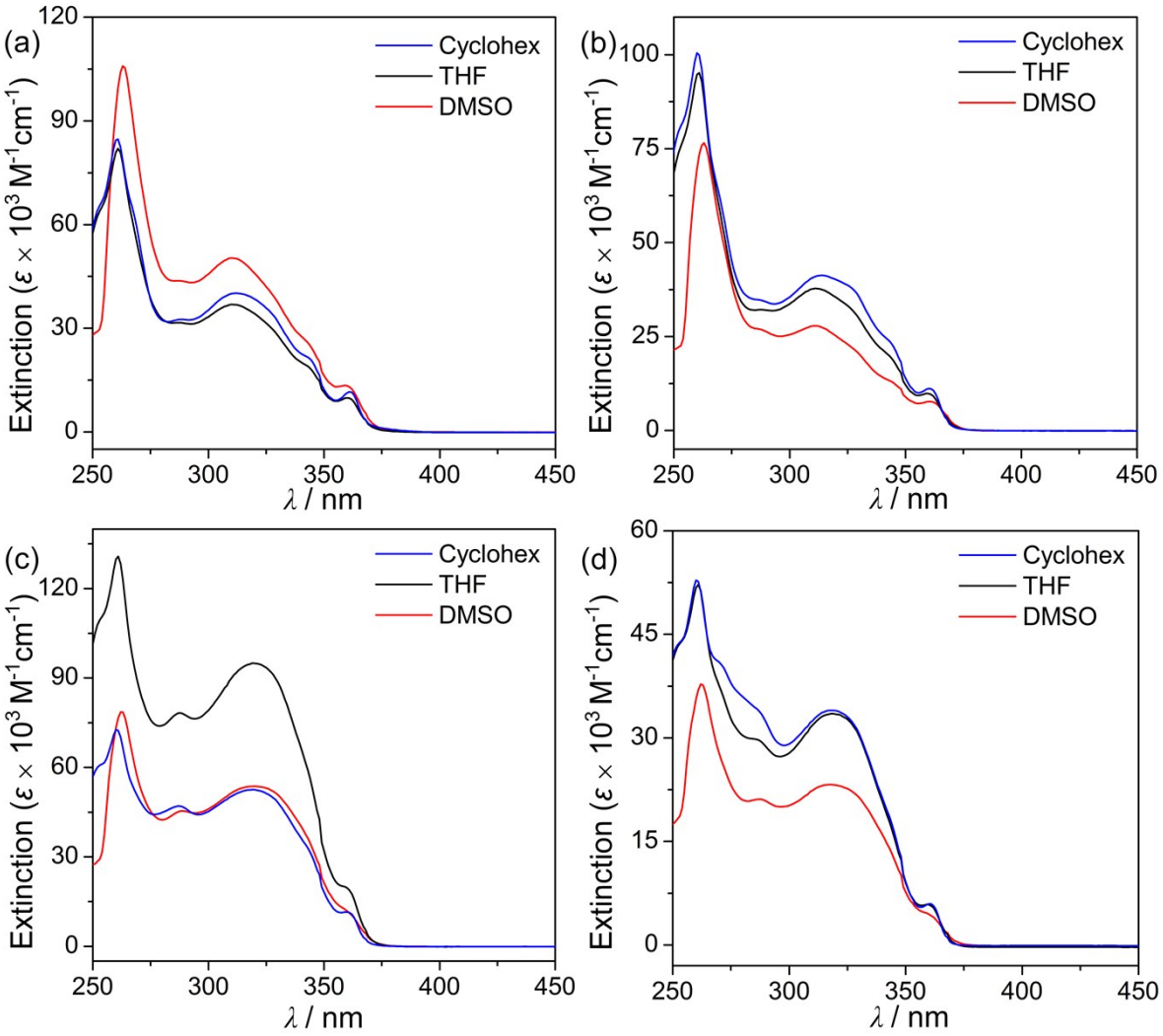

Fig. S1 UV–vis absorption spectra of (a) **1Ph**, (b) **2Ph**, (c) **1BP** and (d) **2BP** in various solvents (2.5×10^{-5} M).

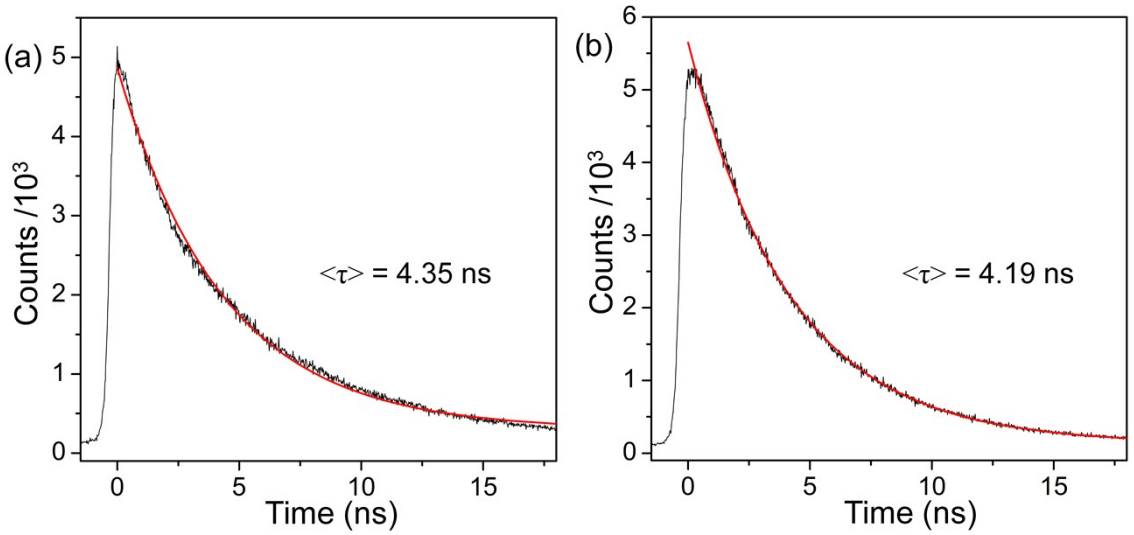

Fig. S2 Emission decay curve detected at (a) 386 nm and (b) 476 nm of THF (5.0×10^{-5} M) solution of **1Ph** at 298 K(black line). The red-line corresponds to the single-exponential fitting curve (R^2 = 0.9968 and 0.9982) for the experimental curve.

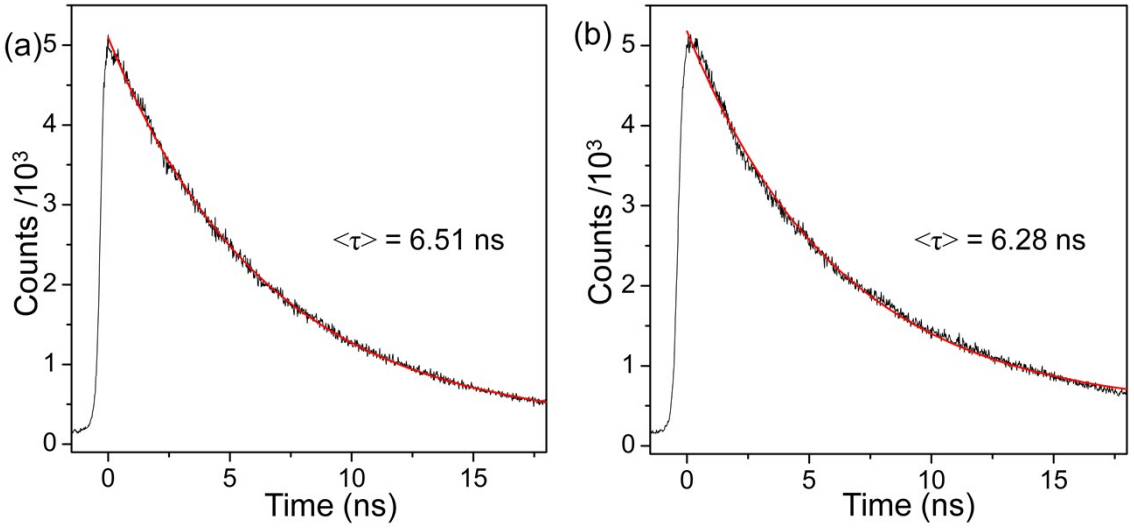

Fig. S3 Emission decay curve detected at (a) 386 nm and (b) 483 nm of THF (5.0×10^{-5} M) solution of **2Ph** at 298 K(black line). The red-line corresponds to the single-exponential fitting curve (R^2 = 0.9985 and 0.9974) for the experimental curve.

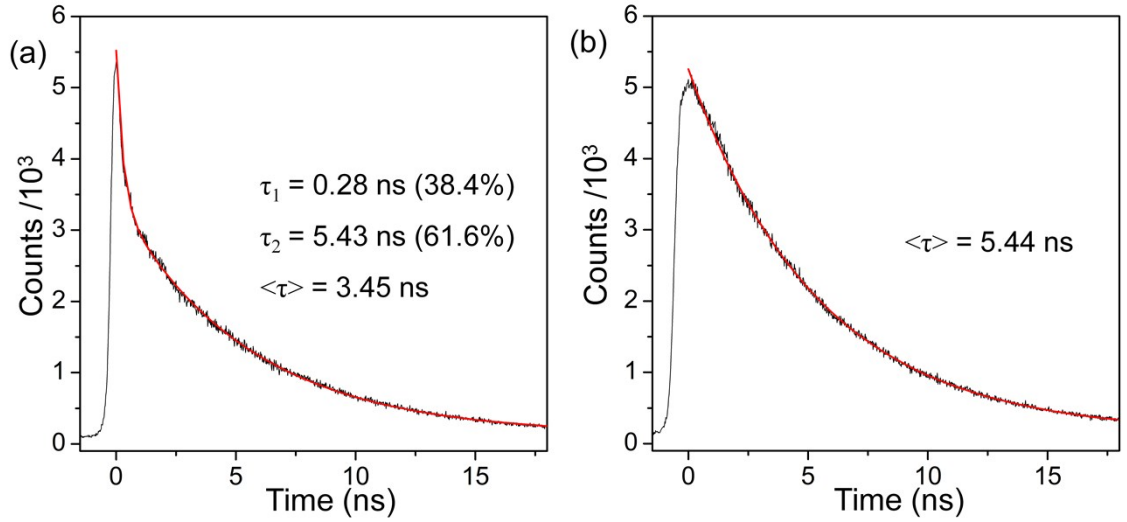

Fig. S4 Emission decay curve detected at (a) 385 nm and (b) 485 nm of THF (5.0×10^{-5} M) solution of **1BP** at 298 K(black line). The red-line corresponds to the double or single-exponential fitting curve (R^2 = 0.9984 and 0.9988) for the experimental curve.

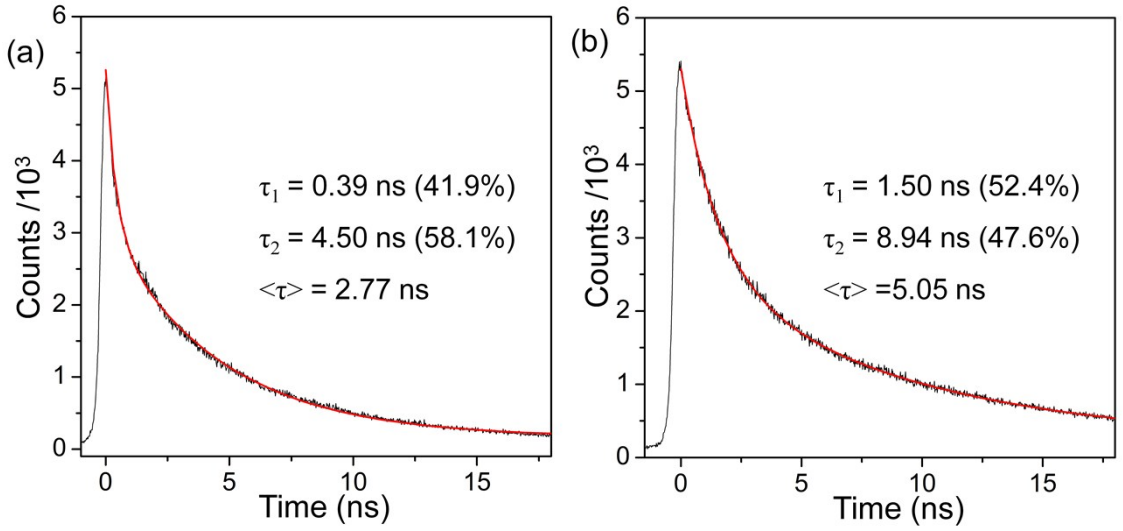

Fig. S5 Emission decay curve detected at (a) 386 nm and (b) 476 nm of THF (5.0×10^{-5} M) solution of **2BP** at 298 K(black line). The red-line corresponds to the double-exponential fitting curve (R^2 = 0.9984 and 0.9984) for the experimental curve.

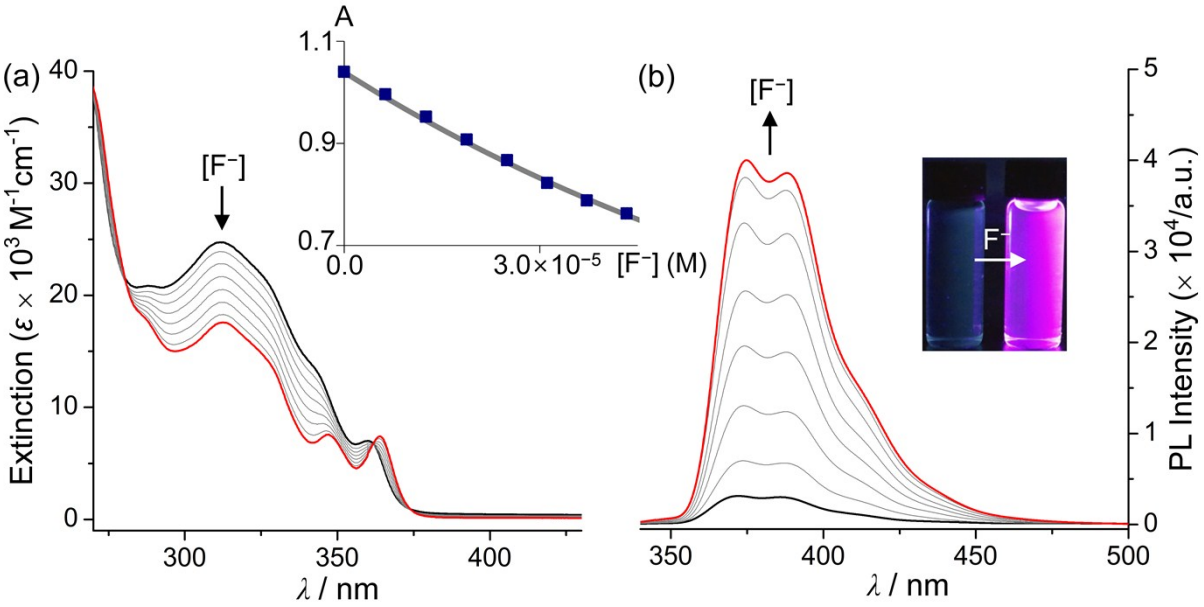

Fig. S6 Spectral change in the (a) UV–vis absorption and (b) PL intensity of a solution **2Ph** (λ_{ex} = 325 nm) in THF (4.00 ×10^{-5} M) upon the addition of TBAF (0–4.30 ×10^{-5} M). The inset shows the absorbance at 311 nm as a function of [F^-]. The line corresponds to the binding isotherm calculated with K = 1.1 ×10^4 M^{-1}

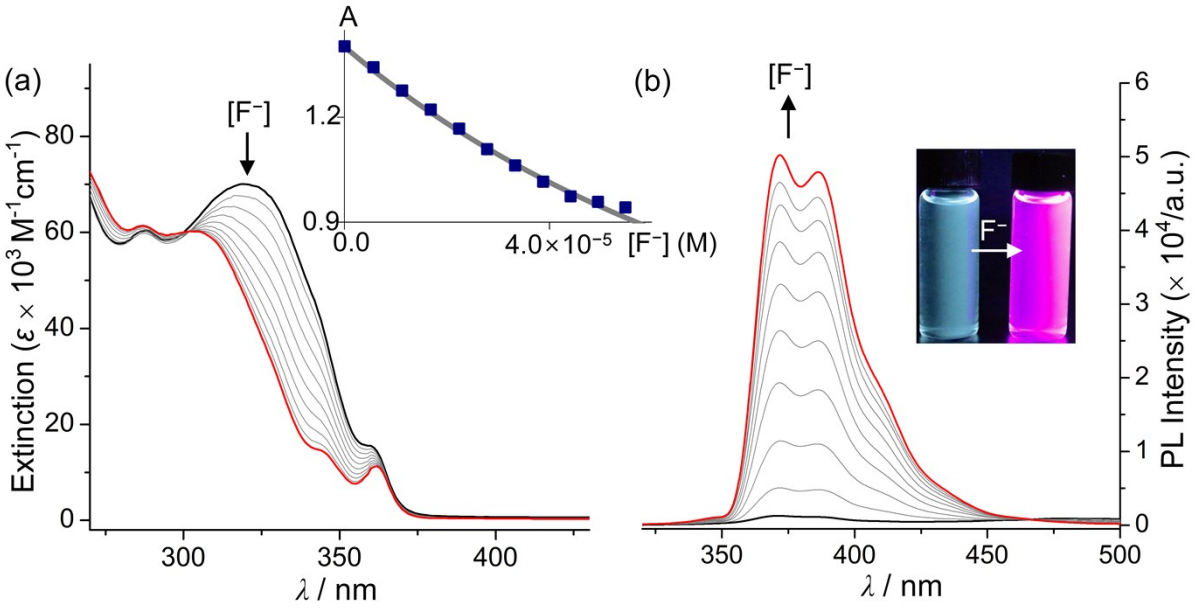

Fig. S7 Spectral change in the (a) UV–vis absorption and (b) PL intensity of a solution **1BP** (λ_{ex} = 296 nm) in THF (2.00 ×10^{-5} M) upon the addition of TBAF (0–5.48 ×10^{-5} M). The inset shows the absorbance at 319 nm as a function of [F^-]. The line corresponds to the binding isotherm calculated with K = 1.0 ×10^4 M^{-1}

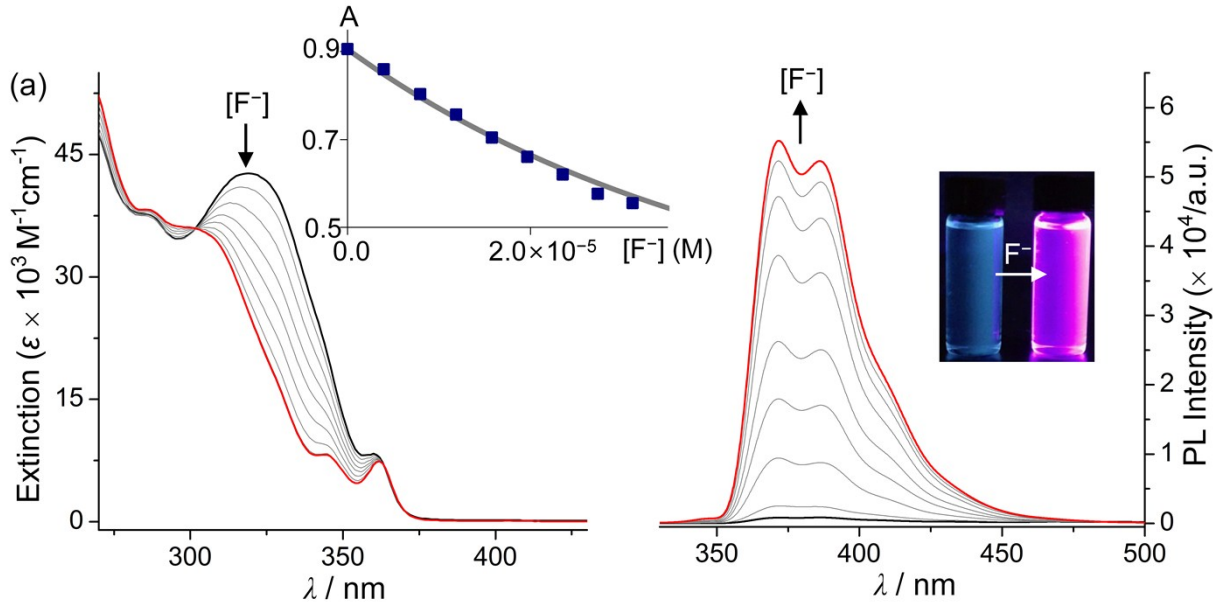

Fig. S8 Spectral change in the (a) UV–vis absorption and (b) PL intensity of a solution **2BP** (λ_{ex} = 292 nm) in THF (2.00 $\times 10^{-5}$ M) upon the addition of TBAF (0–3.1 $\times 10^{-5}$ M). The inset shows the absorbance at 319 nm as a function of [F⁻]. The line corresponds to the binding isotherm calculated with K = 3.0 $\times 10^{4}$ M^{-1}

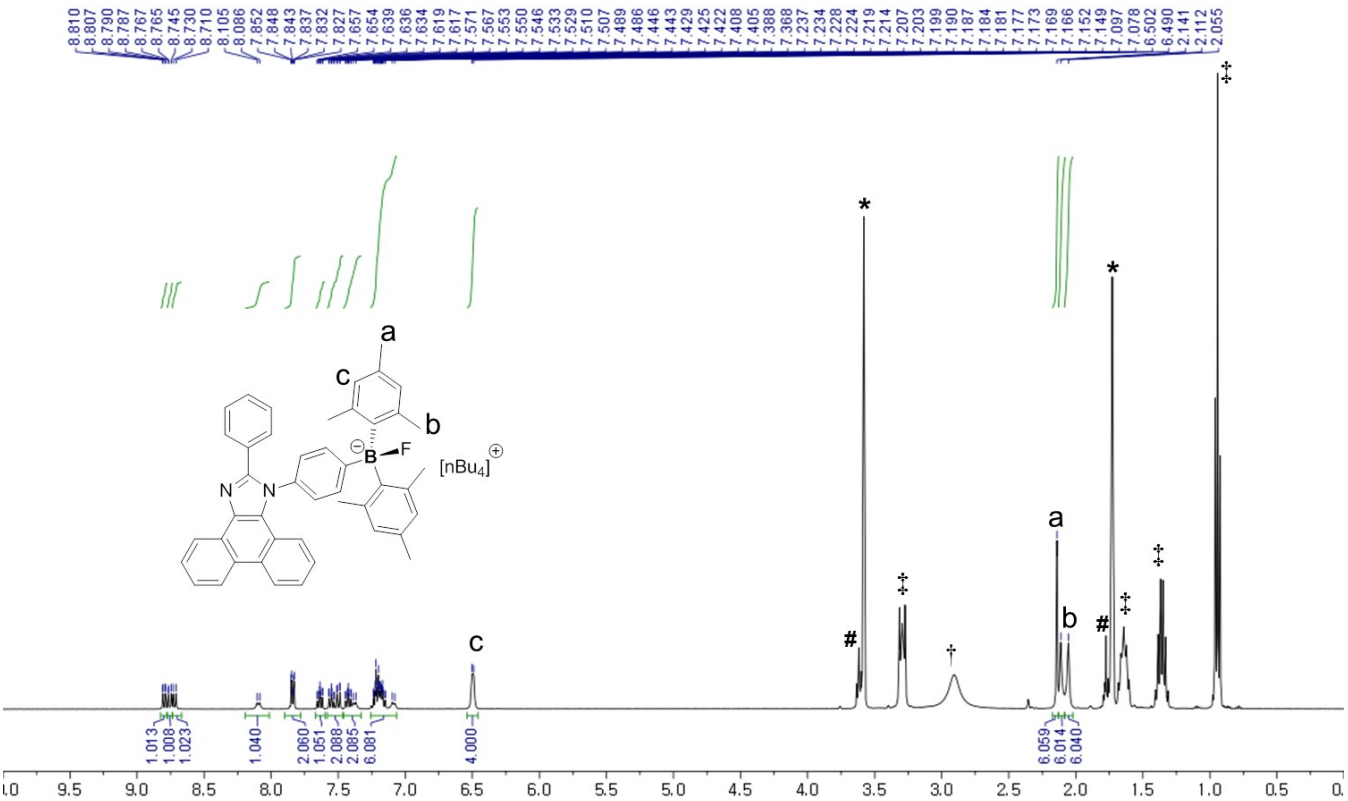

Fig. S9 ^{1}H NMR spectra of **1Ph** with 1.5 equiv TBAF in THF-*d*8. (∗ from THF-*d*8, # from residual THF in THF-*d*8, † from H_2O, and ‡ from *n*Bu).

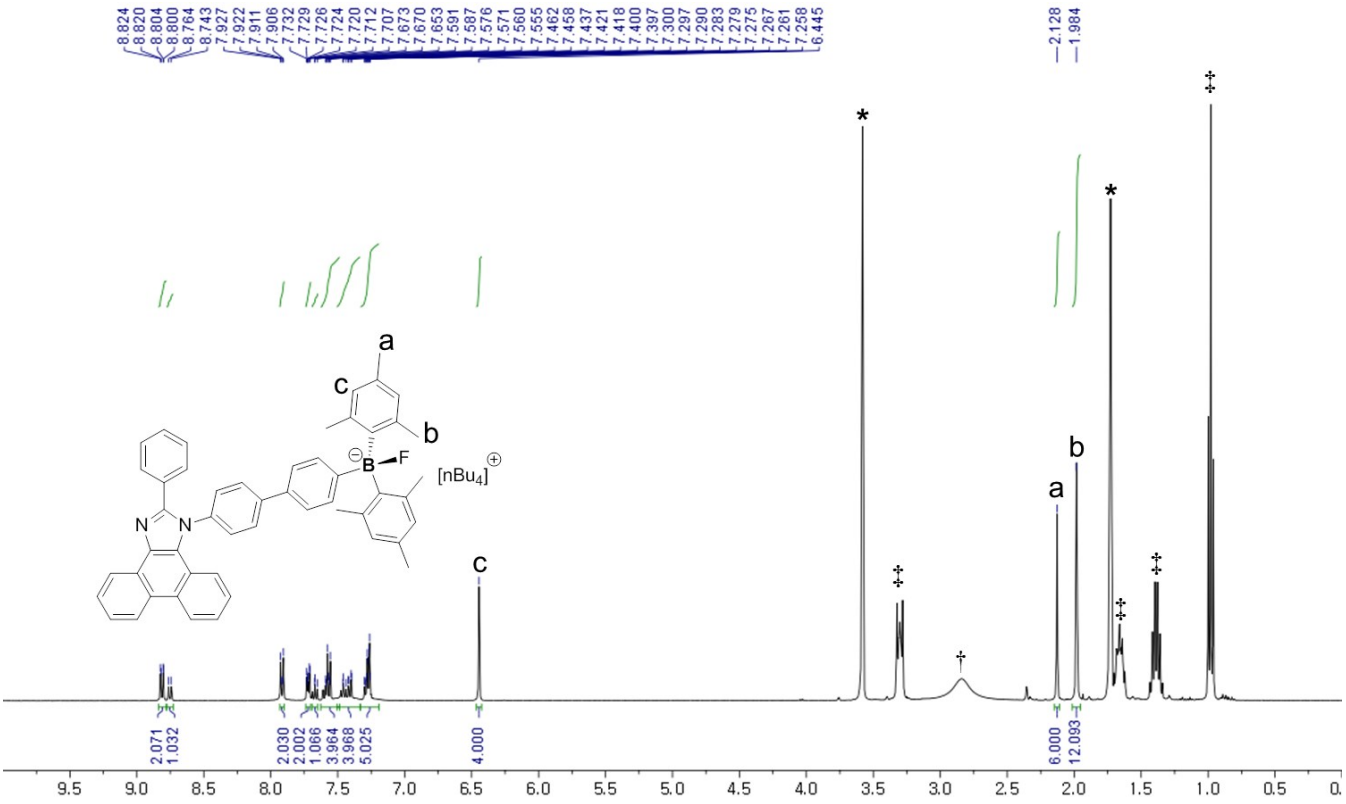

Fig. S10 ^{1}H NMR spectra of **1BP** with 1.5 equiv TBAF in THF-*d*8. (∗ from THF-*d*8, † from H_2O, and ‡ from *n*Bu).

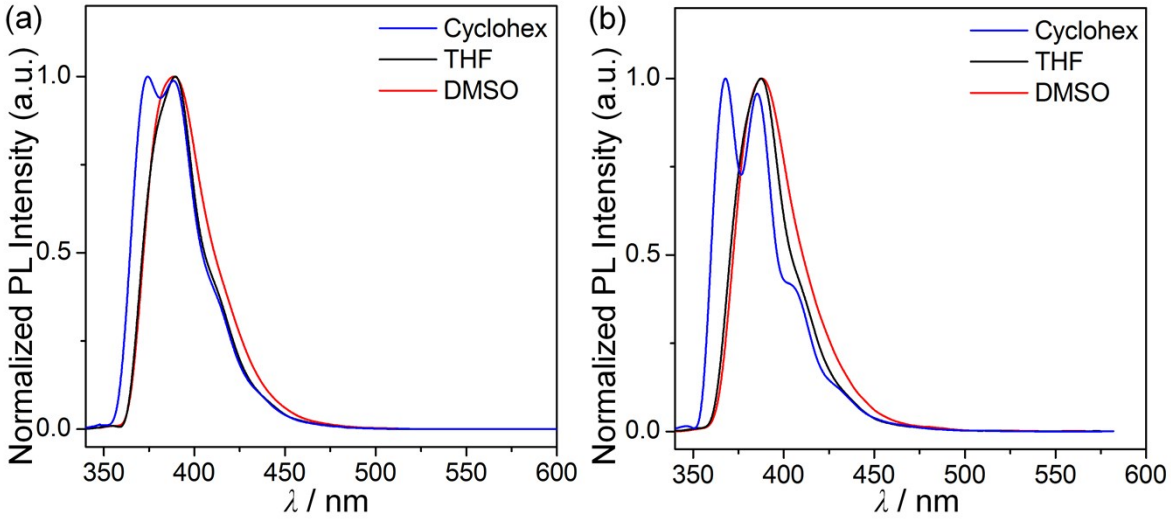

Fig. S11 The PL emission spectra of (a) [**1Ph** + 1.5 equiv. Bu_4NF] (λ_{ex} = 326 nm) and (b) [**1BP** + 1.5 equiv. Bu_4NF] (λ_{ex} = 296 nm) in various organic solvents at 298 K.

Computational details

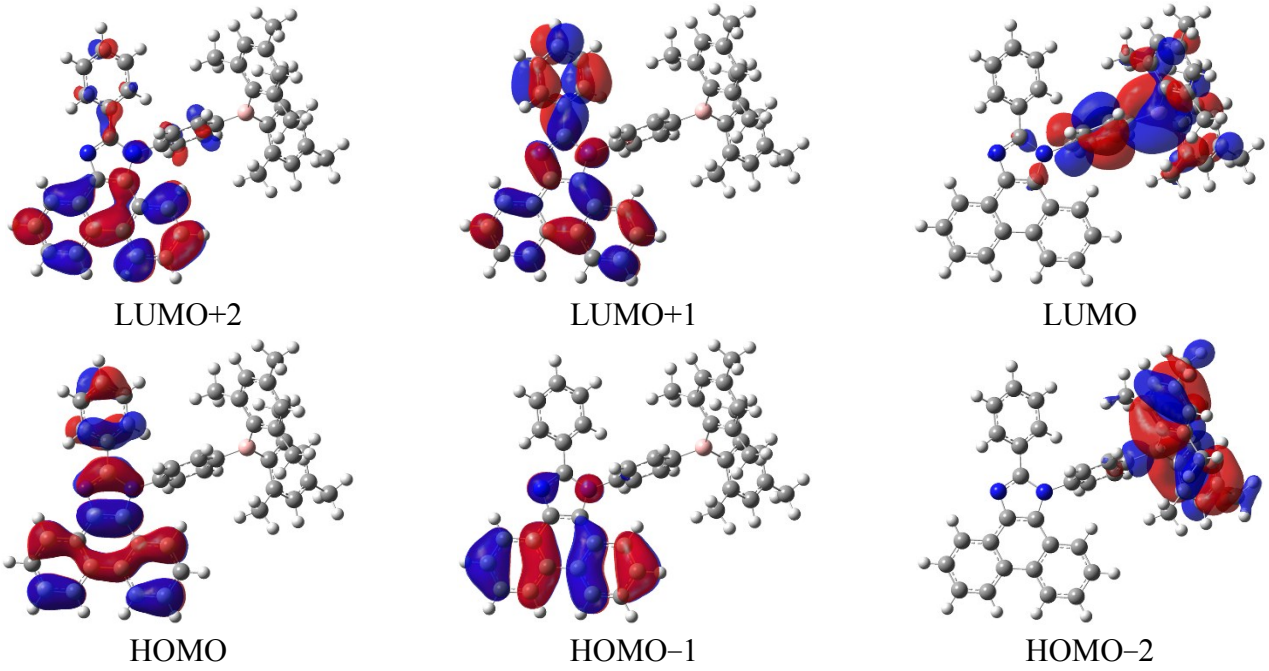

Fig. S12 Frontier molecular orbitals of **1Ph** from B3LYP/6-31G(d) calculations (Isovalue = 0.04) with CPCM in THF at the ground state (S_0) optimized geometries.

Table S3. Computed absorption wavelengths (λ_{calc} in nm) and oscillator strengths ($f_{calc.}$) for **1Ph** from TD-B3LYP/6-31G(d) calculations in THF at the ground state (S_0) optimized geometries

state	λ /nm	f_{calc}	major contribution
1	414.75	0.0088	HOMO → LUMO (99.2%)
2	362.34	0.1090	HOMO−2 → LUMO (98.4%)
3	346.20	0.0687	HOMO−3 → LUMO (98.0%)
4	338.21	0.0530	HOMO−4 → LUMO (25.2%)
			HOMO−1 → LUMO (64.9%)
5	336.59	0.0928	HOMO−4 → LUMO (71.2%)
			HOMO−1 → LUMO (17.1%)
6	333.06	0.2510	HOMO−5 → LUMO (12.1%)
			HOMO−1 → LUMO (15.8%)
			HOMO → LUMO+1 (53.5%)
			HOMO → LUMO+2 (11.2%)

Table S4. Molecular orbital energies (in eV) and distributions (in %) of **1Ph** at the ground state (S_0) optimized geometries

	E (eV)	Phenanthro -imidazole	dimesitylborane	bridged phenyl
LUMO+2	−0.93	94.3	1.2	4.5
LUMO+1	−1.19	98.2	1.0	0.8
LUMO	−1.98	2.4	61.9	35.6
HOMO	−5.44	99.6	0.0	0.4
HOMO−1	−6.07	99.3	0.1	0.6
HOMO−2	−6.19	0.0	95.6	4.4

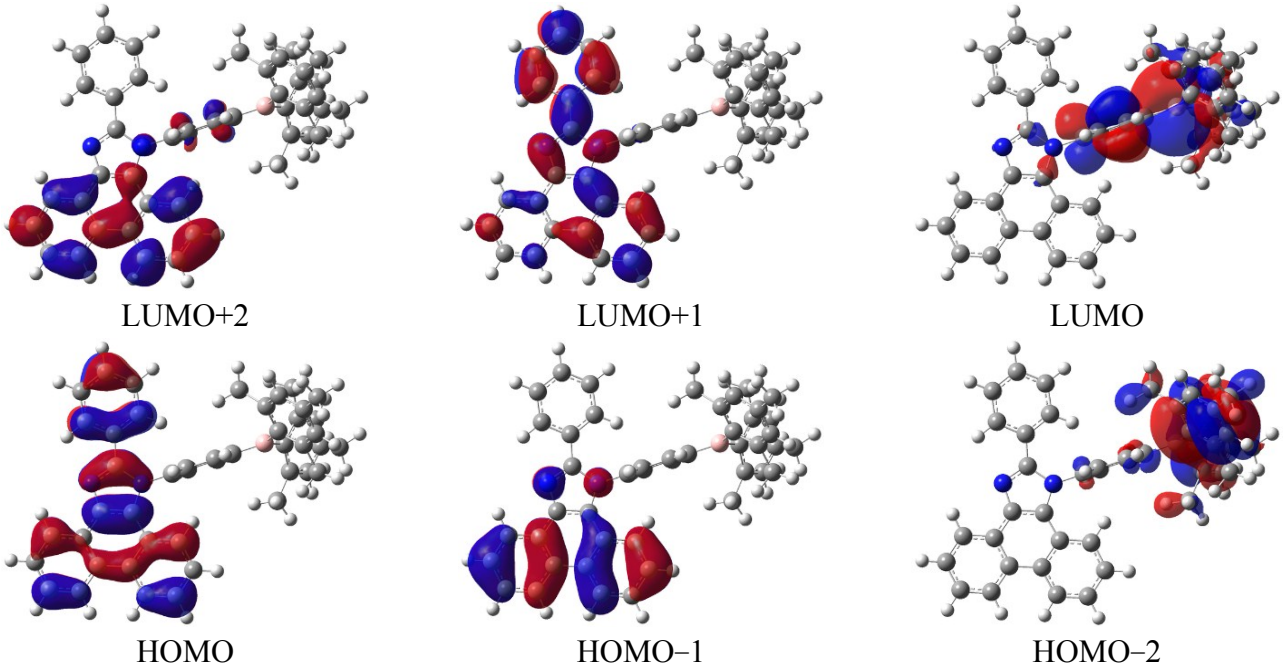

Fig. S13 Frontier molecular orbitals of **1Ph** from B3LYP/6-31G(d) calculations (Isovalue = 0.04) with CPCM in THF at the first excited state (S_1) optimized geometries.

Table S5. Computed absorption wavelengths (λ_{calc} in nm) and oscillator strengths ($f_{calc.}$) for **1Ph** from TD-B3LYP/6-31G(d) calculations in THF at the first excited state (S_1) optimized geometries

state	λ /nm	f_{calc}	major contribution
1	520.27	0.0003	HOMO → LUMO (99.4%)
2	394.13	0.0695	HOMO−3 → LUMO (87.3%)
			HOMO−2 → LUMO (11.4%)
3	388.47	0.0691	HOMO−3 → LUMO (11.2%)
			HOMO−2 → LUMO (85.6%)
4	373.95	0.0758	HOMO−4 → LUMO (98.6%)
5	367.43	0.0017	HOMO−1 → LUMO (97.2%)
6	363.20	0.0076	HOMO−5 → LUMO (95.7%)
7	361.20	0.7249	HOMO → LUMO+1 (88.7%)

Table S6. Molecular orbital energies (in eV) and distributions (in %) of **1Ph** at the first excited state (S_1) optimized geometries

	E (eV)	Phenanthro -imidazole	dimesitylborane	bridged phenyl
LUMO+2	−0.92	95.4	0.1	4.5
LUMO+1	−1.37	99.2	0.1	0.7
LUMO	−2.32	2.1	50.2	47.7
HOMO	−5.21	99.8	0.0	0.2
HOMO−1	−6.13	98.9	0.7	0.4
HOMO−2	−6.23	0.9	96.2	2.9

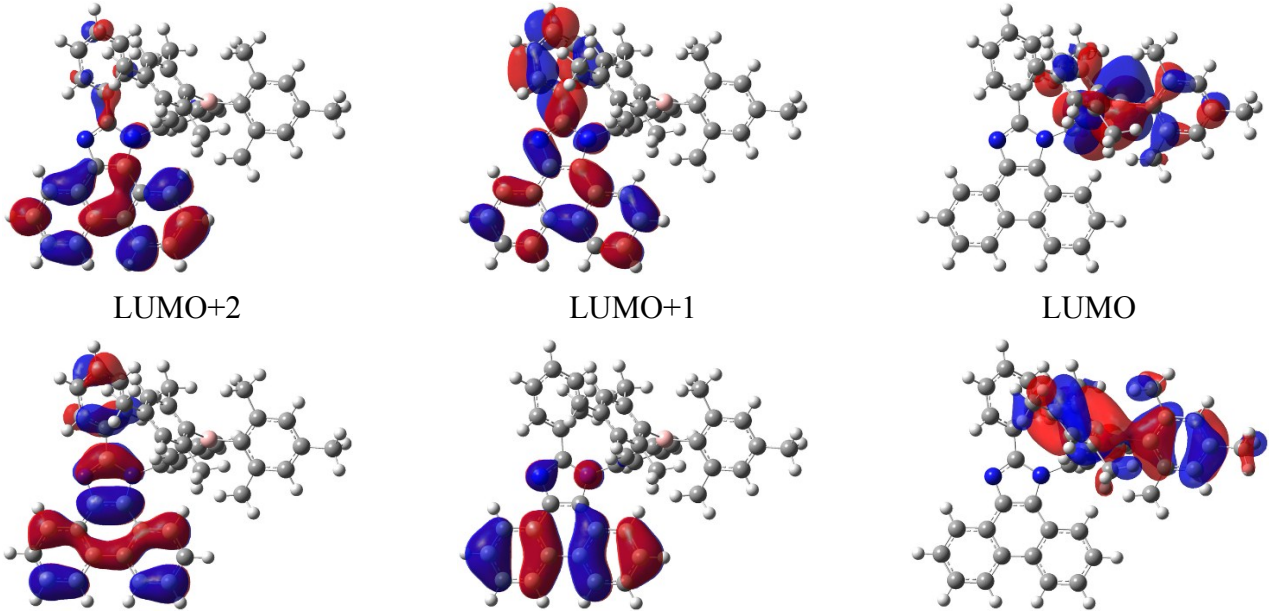

Fig. S14 Frontier molecular orbitals of **2Ph** from B3LYP/6-31G(d) calculations (Isovalue = 0.04) with CPCM in THF at the ground state (S_0) optimized geometries.

Table S7. Computed absorption wavelengths (λ_{calc} in nm) and oscillator strengths ($f_{calc.}$) for **2Ph** from TD-B3LYP/6-31G(d) calculations in THF at the ground state (S_0) optimized geometries

state	λ /nm	f_{calc}	major contribution
1	410.42	0.0011	HOMO → LUMO (99.5%)
2	360.11	0.1043	HOMO−2 → LUMO (94.6%)
3	344.23	0.0416	HOMO−3 → LUMO (96.9%)
4	335.77	0.0763	HOMO−4 → LUMO (92.6%)
5	334.62	0.0064	HOMO−1 → LUMO (89.6%)
6	332.62	0.3004	HOMO → LUMO+1 (71.0%)
			HOMO → LUMO+2 (17.5%)

Table S8. Molecular orbital energies (in eV) and distributions (in %) of **2Ph** at the ground state (S_0) optimized geometries

	E (eV)	Phenanthro -imidazole	dimesitylborane	bridged phenyl
LUMO+2	−0.91	97.7	1.3	1.0
LUMO+1	−1.16	98.9	0.4	0.7
LUMO	−1.94	1.1	63.1	35.9
HOMO	−5.44	99.7	0.0	0.3
HOMO−1	−6.06	98.1	1.3	0.6
HOMO−2	−6.19	1.7	94.1	4.3

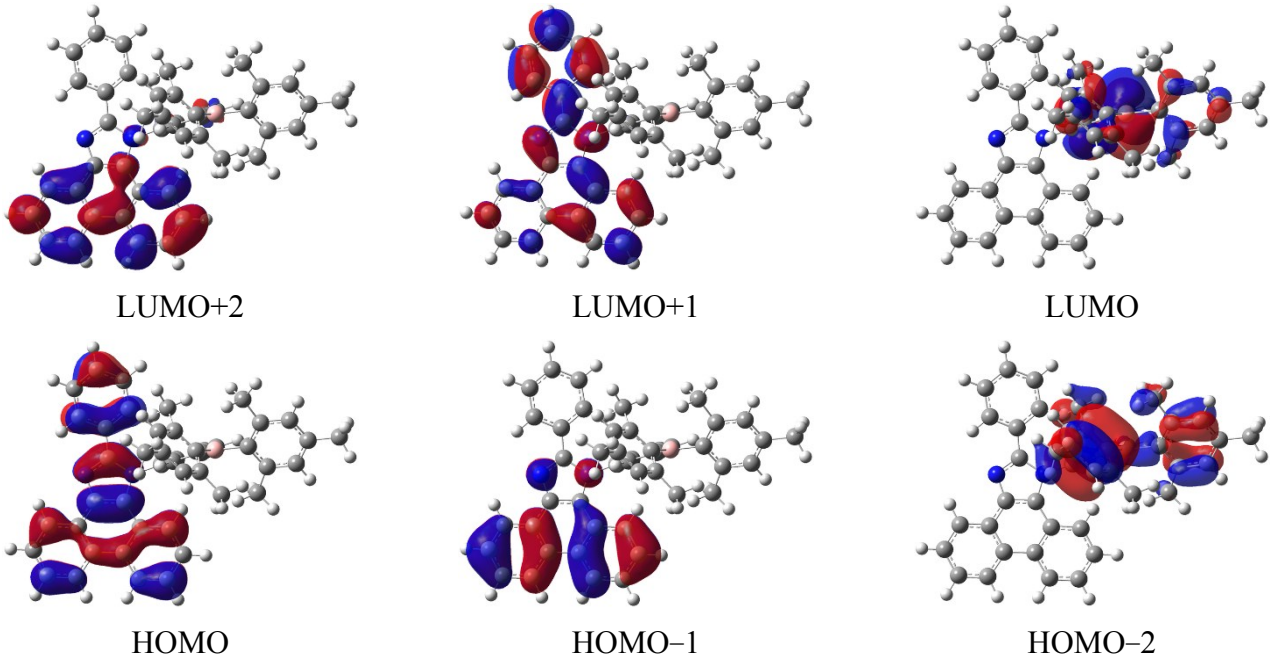

Fig. S15 Frontier molecular orbitals of **2Ph** from B3LYP/6-31G(d) calculations (Isovalue = 0.04) with CPCM in THF at the first excited state (S_1) optimized geometries.

Table S9. Computed absorption wavelengths (λ_{calc} in nm) and oscillator strengths ($f_{calc.}$) for **2Ph** from TD-B3LYP/6-31G(d) calculations in THF at the first excited state (S_1) optimized geometries

state	λ /nm	f_{calc}	major contribution
1	522.86	0.0003	HOMO → LUMO (99.7%)
2	394.18	0.0678	HOMO−3 → LUMO (51.2%)
			HOMO−2 → LUMO (43.9%)
3	387.13	0.0488	HOMO−3 → LUMO (44.7%)
			HOMO−2 → LUMO (53.0%)
4	374.43	0.0646	HOMO−4 → LUMO (97.7%)
5	369.10	0.0004	HOMO−1 → LUMO (95.9%)
6	363.62	0.0068	HOMO−5 → LUMO (95.3%)
7	360.37	0.6975	HOMO → LUMO+1 (88.0%)

Table S10. Molecular orbital energies (in eV) and distributions (in %) of **2Ph** at the first excited state (S_1) optimized geometries

	E (eV)	Phenanthro -imidazole	dimesitylborane	bridged phenyl
LUMO+2	−0.89	97.6	0.5	1.9
LUMO+1	−1.33	99.2	0.1	0.7
LUMO	−2.31	1.1	51.0	47.9
HOMO	−5.19	99.8	0.0	0.1
HOMO−1	−6.11	98.5	1.1	0.5
HOMO−2	−6.22	0.7	96.6	2.6

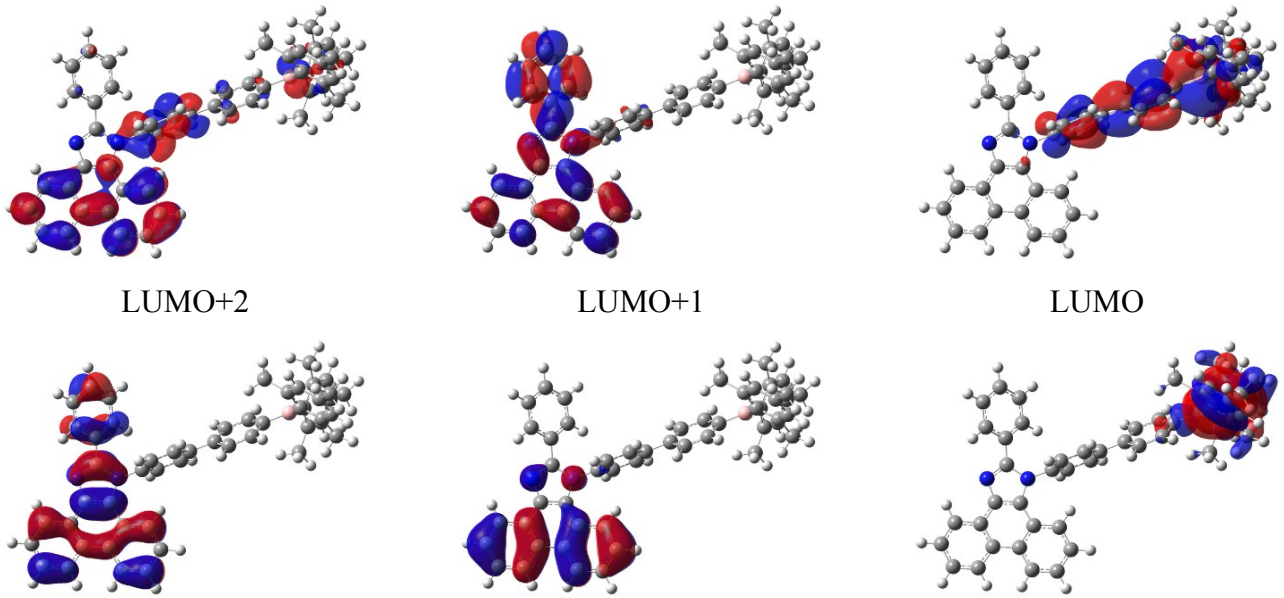

Fi. S16 Frontier molecular orbitals of **1BP** from B3LYP/6-31G(d) calculations (Isovalue = 0.04) with CPCM in THF at the ground state (S_0) optimized geometries.

Table S11. Computed absorption wavelengths (λ_{calc} in nm) and oscillator strengths ($f_{calc.}$) for **1BP** from TD-B3LYP/6-31G(d) calculations in THF at the ground state (S_0) optimized geometries

state	λ /nm	f_{calc}	major contribution
1	395.98	0.0117	HOMO → LUMO (98.2%)
2	361.18	0.0977	HOMO−2 → LUMO (97.3%)
3	349.44	0.3012	HOMO−3 → LUMO (94.5%)
4	337.96	0.1293	HOMO−4 → LUMO (95.6%)
5	333.26	0.3213	HOMO → LUMO+1 (66.5%)
			HOMO → LUMO+2 (20.0%)

Table S12. Molecular orbital energies (in eV) and distributions (in %) of **1BP** at the ground state (S_0) optimized geometries

	E (eV)	Phenanthro -imidazole	dimesitylborane	bridged phenyl
LUMO+2	−0.96	76.3	6.7	17.1
LUMO+1	−1.18	96.4	1.1	2.4
LUMO	−1.97	0.9	51.0	48.1
HOMO	−5.44	99.5	0.0	0.4
HOMO−1	−6.07	97.8	0.4	1.8
HOMO−2	−6.15	0.0	95.4	4.6

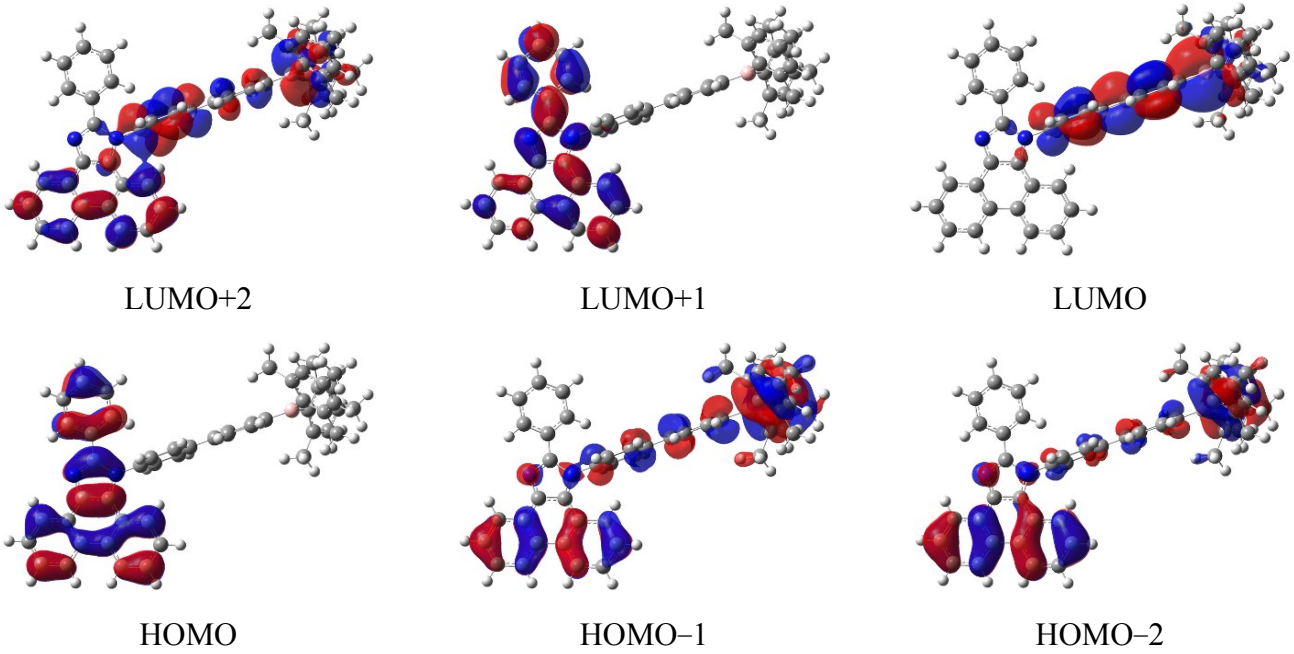

Fig. S17 Frontier molecular orbitals of **1BP** from B3LYP/6-31G(d) calculations (Isovalue = 0.04) with CPCM in THF at the first excited state (S_1) optimized geometries.

Table S13. Computed absorption wavelengths (λ_{calc} in nm) and oscillator strengths ($f_{calc.}$) for **1BP** from TD-B3LYP/6-31G(d) calculations in THF at the first excited state (S_1) optimized geometries

state	λ /nm	f_{calc}	major contribution
1	508.14	0.0024	HOMO → LUMO (98.9%)
2	397.60	0.0596	HOMO−3 → LUMO (95.2%)
3	396.57	0.3694	HOMO−2 → LUMO (30.7%)
			HOMO−1 → LUMO (61.2%)
4	378.74	0.1220	HOMO−4 → LUMO (95.4%)
5	365.06	0.0045	HOMO−5 → LUMO (98.3%)
6	364.59	0.0082	HOMO−2 → LUMO (65,1%)
			HOMO−1 → LUMO (32.3%)
7	359.61	0.7675	HOMO → LUMO+1 (89.8%)

Table S14. Molecular orbital energies (in eV) and distributions (in %) of **1BP** at the first excited state (S_1) optimized geometries

	E (eV)	Phenanthro -imidazole	dimesitylborane	bridged phenyl
LUMO+2	−0.95	39.3	24.7	36.1
LUMO+1	−1.34	98.9	0.2	0.9
LUMO	−2.38	1.1	34.2	64.7
HOMO	−5.21	99.8	0.0	0.2
HOMO−1	−6.11	35.6	43.3	21.1
HOMO−2	−6.13	64.8	26.5	8.6

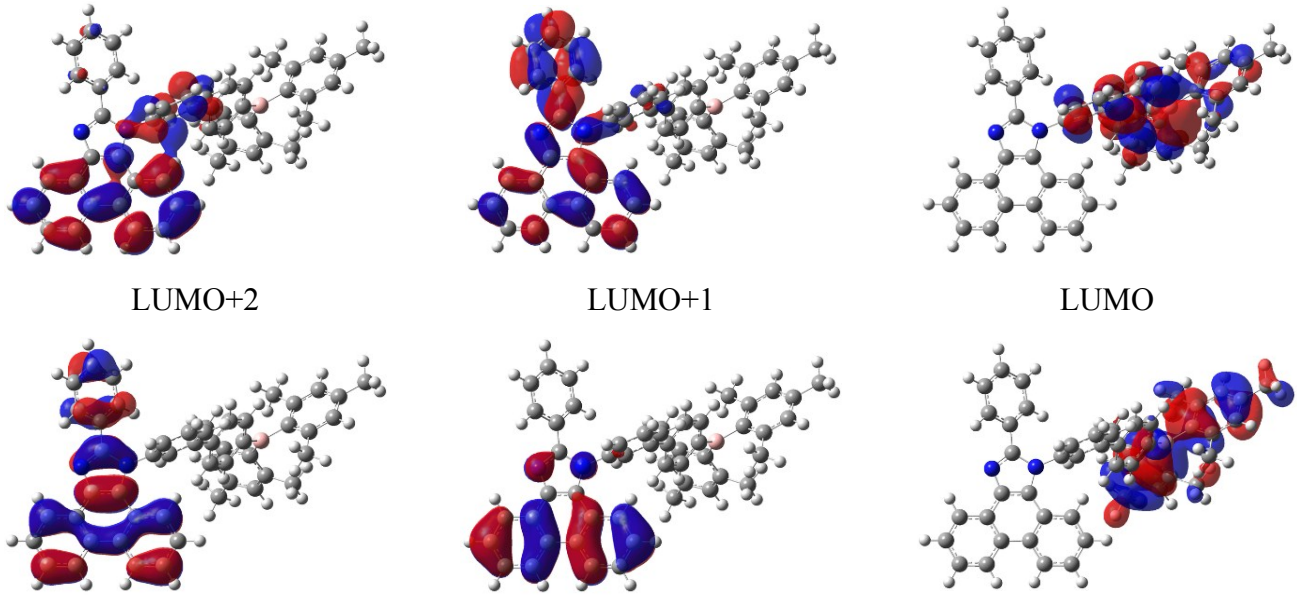

Fig. S18 Frontier molecular orbitals of **2BP** from B3LYP/6-31G(d) calculations (Isovalue = 0.04) with CPCM in THF at the ground state (S_0) optimized geometries.

Table S15. Computed absorption wavelengths (λ_{calc} in nm) and oscillator strengths ($f_{calc.}$) for **2BP** from TD-B3LYP/6-31G(d) calculations in THF at the ground state (S_0) optimized geometries

state	λ /nm	f_{calc}	major contribution
1	395.64	0.0017	HOMO → LUMO (98.9%)
2	360.69	0.2500	HOMO−2 → LUMO (97.4%)
3	348.05	0.1000	HOMO−3 → LUMO (96.5%)
4	336.35	0.1184	HOMO−4 → LUMO (96.7%)
5	332.89	0.3432	HOMO → LUMO+1 (69.4%)
			HOMO → LUMO+2 (20.8%)

Table S16. Molecular orbital energies (in eV) and distributions (in %) of **2BP** at the ground state (S_0) optimized geometries

	E (eV)	Phenanthro -imidazole	dimesitylborane	bridged phenyl
LUMO+2	−0.96	84.2	1.3	14.4
LUMO+1	−1.18	96.5	0.1	3.4
LUMO	−1.95	0.4	52.5	47.1
HOMO	−5.44	99.6	0.0	0.4
HOMO−1	−6.07	98.7	0.2	1.1
HOMO−2	−6.14	0.0	95.4	4.6

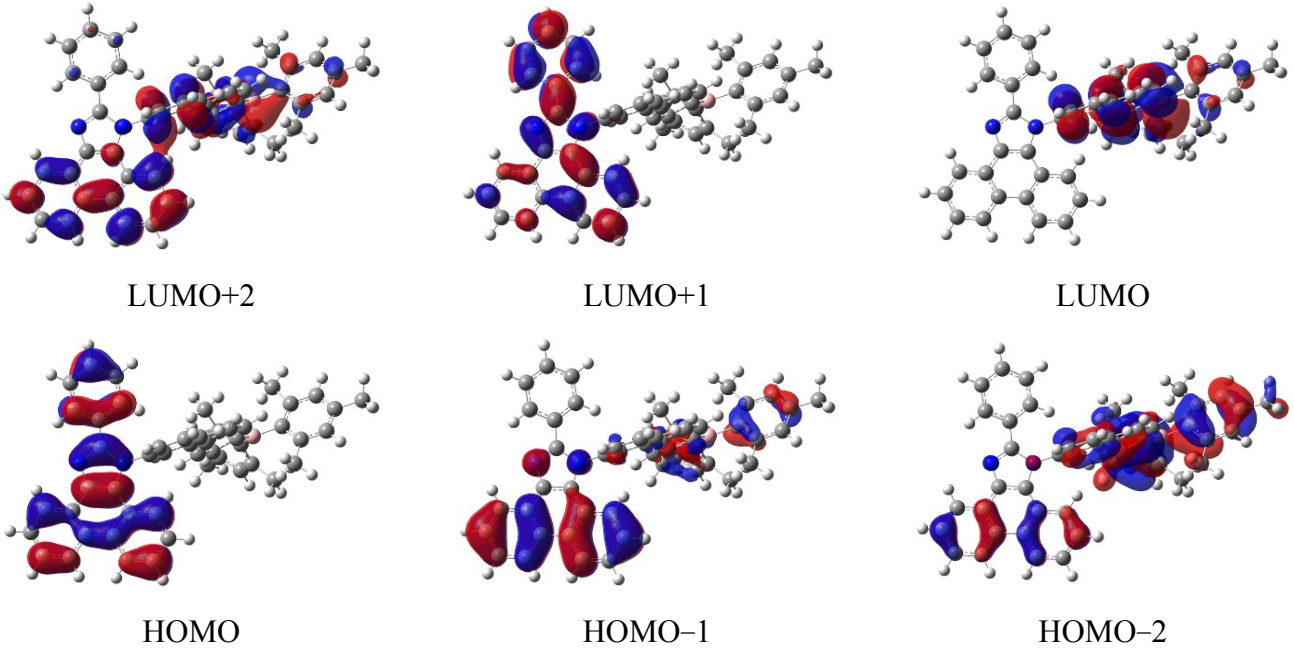

Fig. S19 Frontier molecular orbitals of **2BP** from B3LYP/6-31G(d) calculations (Isovalue = 0.04) with CPCM in THF at the first excited state (S_1) optimized geometries.

Table S17. Computed absorption wavelengths (λ_{calc} in nm) and oscillator strengths ($f_{calc.}$) for **2BP** from TD-B3LYP/6-31G(d) calculations in THF at the first excited state (S_1) optimized geometries

state	λ /nm	f_{calc}	major contribution
1	509.59	0.0008	HOMO → LUMO (99.3%)
2	397.26	0.0533	HOMO−3 → LUMO (97.5%)
3	395.11	0.2832	HOMO−2 → LUMO (77.0%)
			HOMO−1 → LUMO (18.4%)
4	378.34	0.0930	HOMO−4 → LUMO (96.7%)
5	365.29	0.0010	HOMO−2 → LUMO (19.3%)
			HOMO−1 → LUMO (79.7%)
6	364.58	0.0031	HOMO−5 → LUMO (98.3%)
7	359.76	0.7166	HOMO → LUMO+1 (90.9%)

Table S18. Molecular orbital energies (in eV) and distributions (in %) of **2BP** at the first excited state (S_1) optimized geometries

	E (eV)	Phenanthro -imidazole	dimesitylborane	bridged phenyl
LUMO+2	−0.94	53.6	18.1	28.3
LUMO+1	−1.33	99.1	0.0	0.9
LUMO	−2.36	0.5	35.3	64.2
HOMO	−5.20	99.8	0.0	0.2
HOMO−1	−6.11	81.5	12.8	5.6
HOMO−2	−6.13	18.2	64.3	17.5

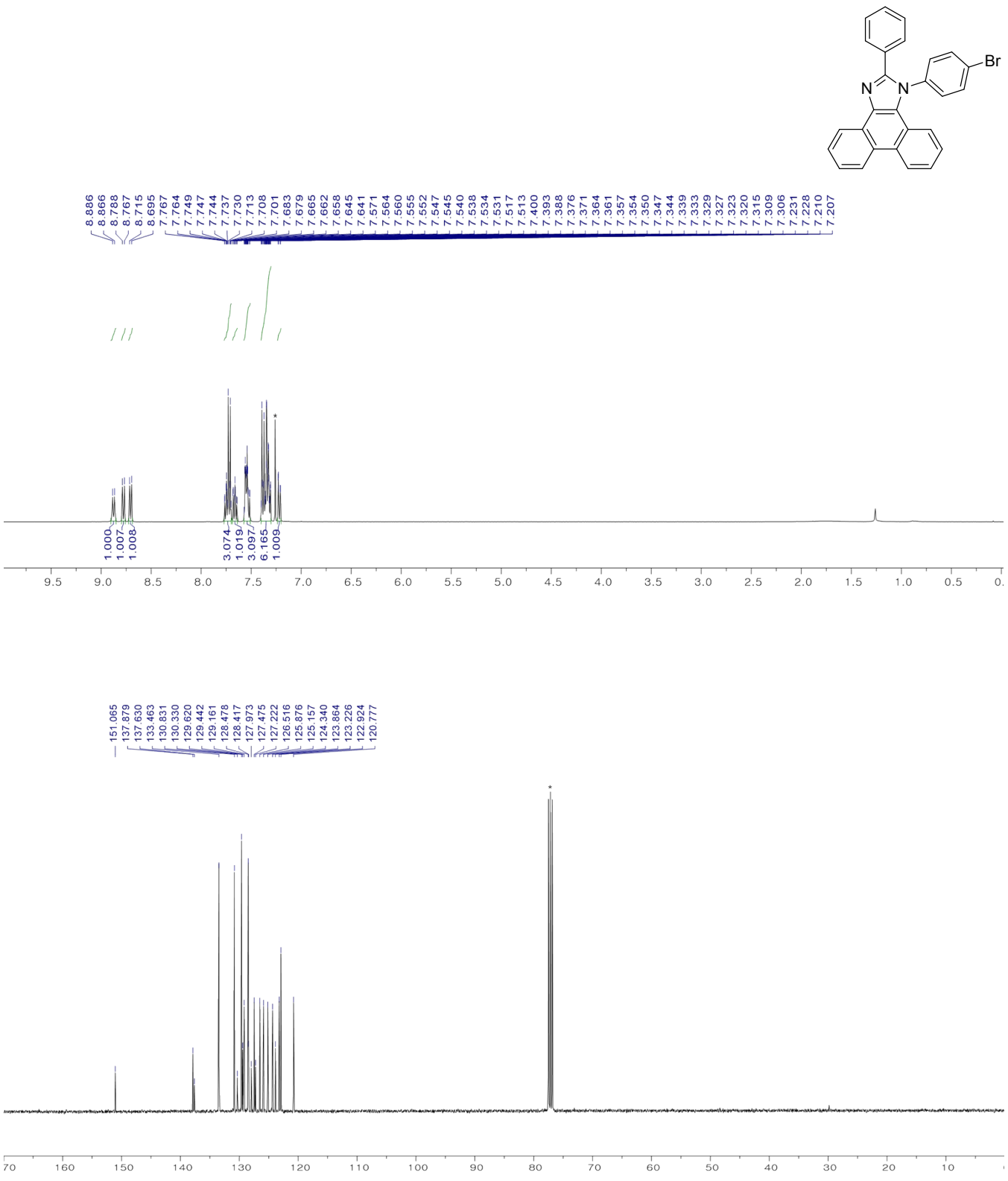

Fig. S20 ^{1}H (top) and ^{13}C (bottom) NMR spectrum of **1a** (∗ from residual $CHCl_3$ in $CDCl_3$).

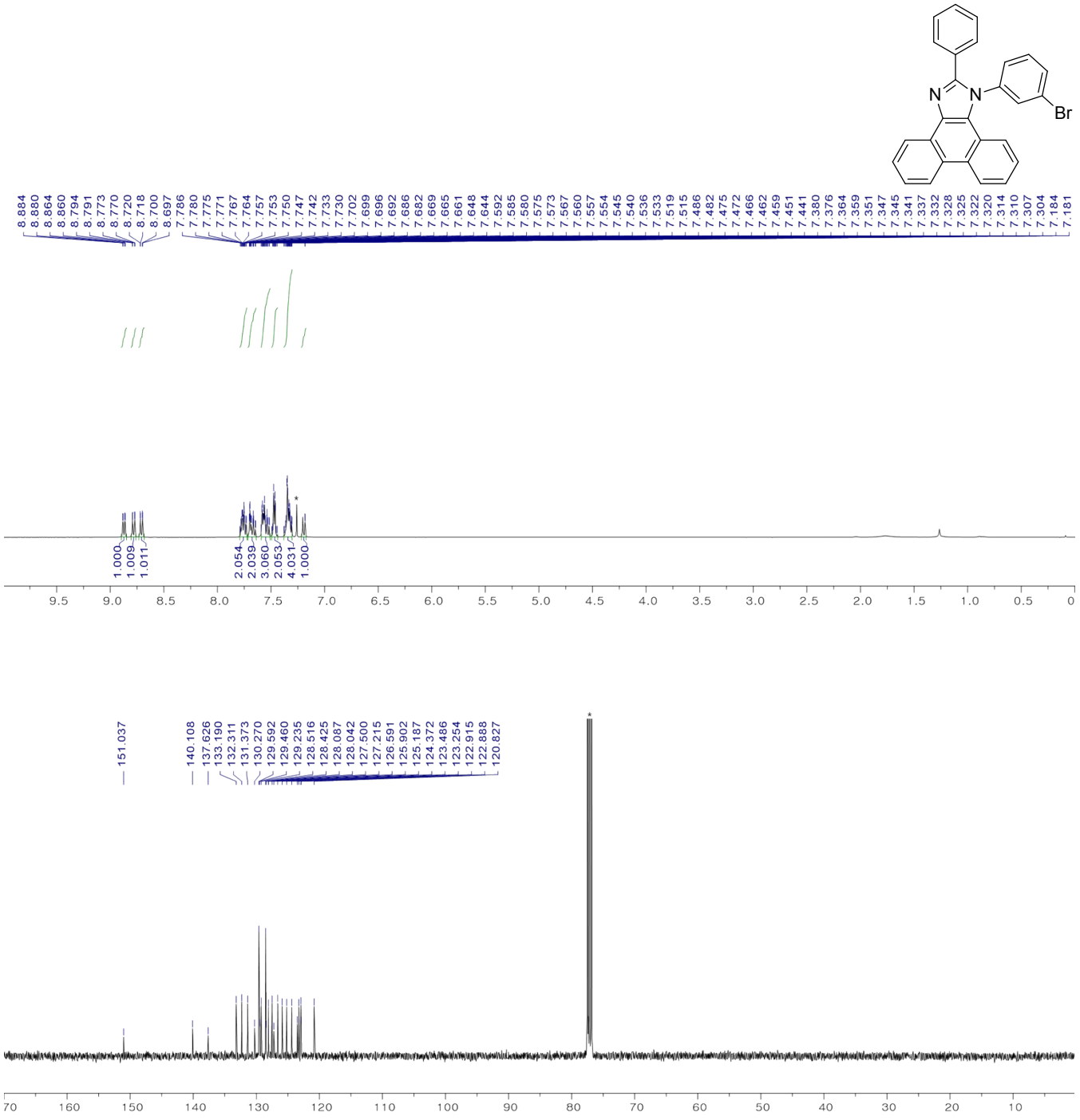

Fig. S21 ^{1}H (top) and ^{13}C (bottom) NMR spectrum of **2a** (∗ from residual $CHCl_3$ in $CDCl_3$).

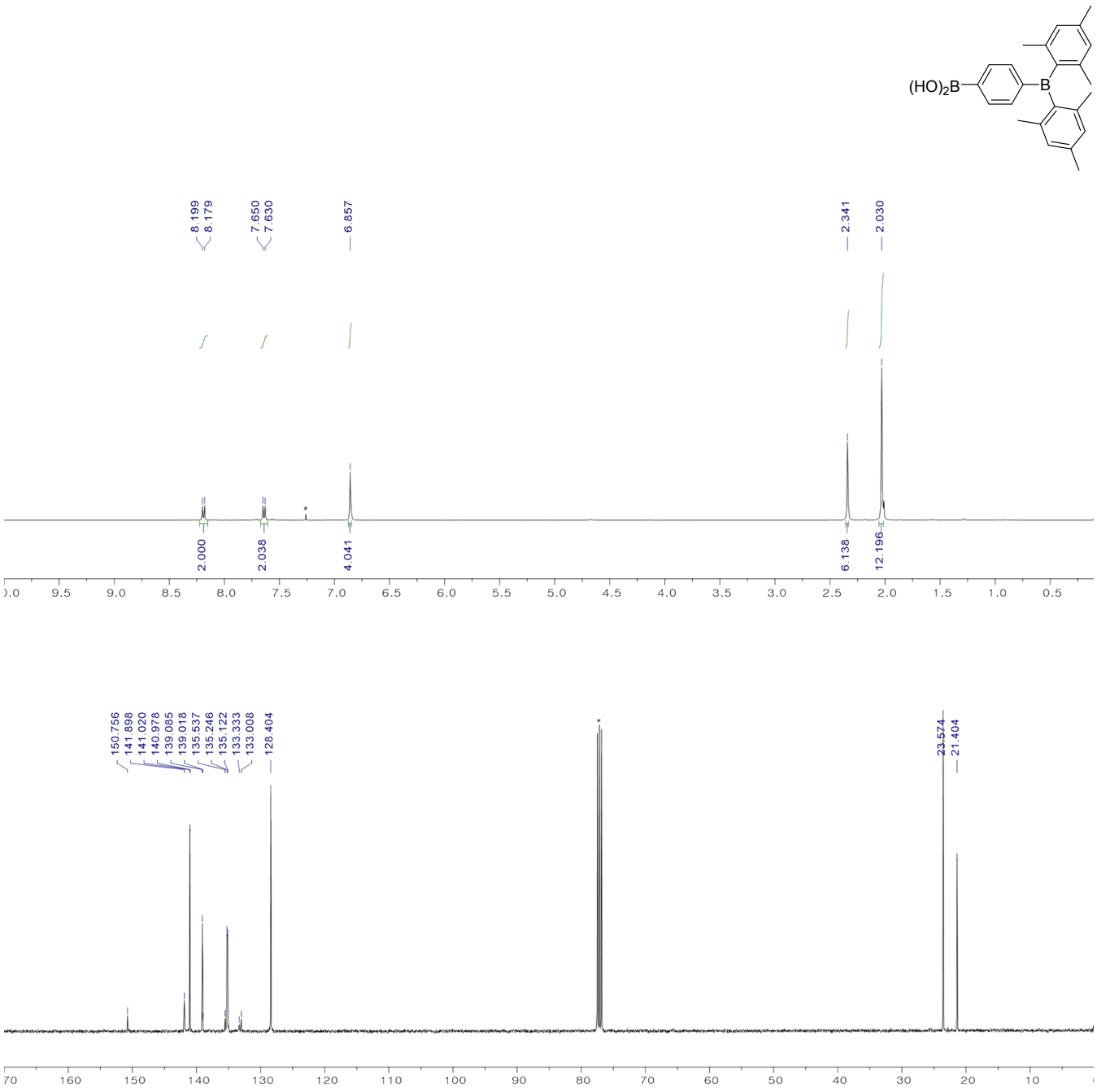

Fig. S22 ^{1}H (top) and ^{13}C (bottom) NMR spectrum of **3a** (∗ from residual $CHCl_3$ in $CDCl_3$).

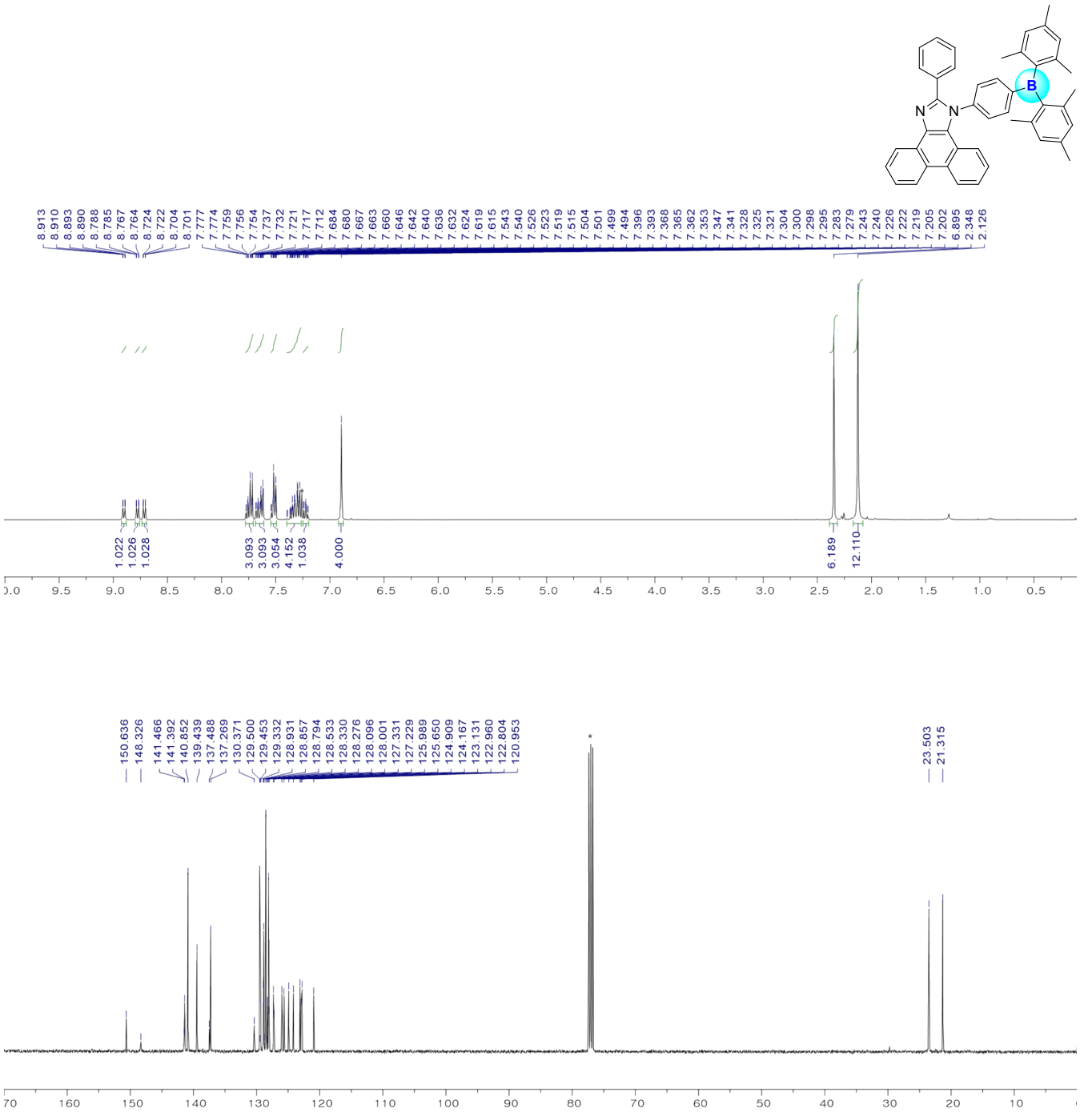

Fig. S23 ^{1}H (top) and ^{13}C (bottom) NMR spectrum of **1Ph** (∗ from residual $CHCl_3$ in $CDCl_3$).

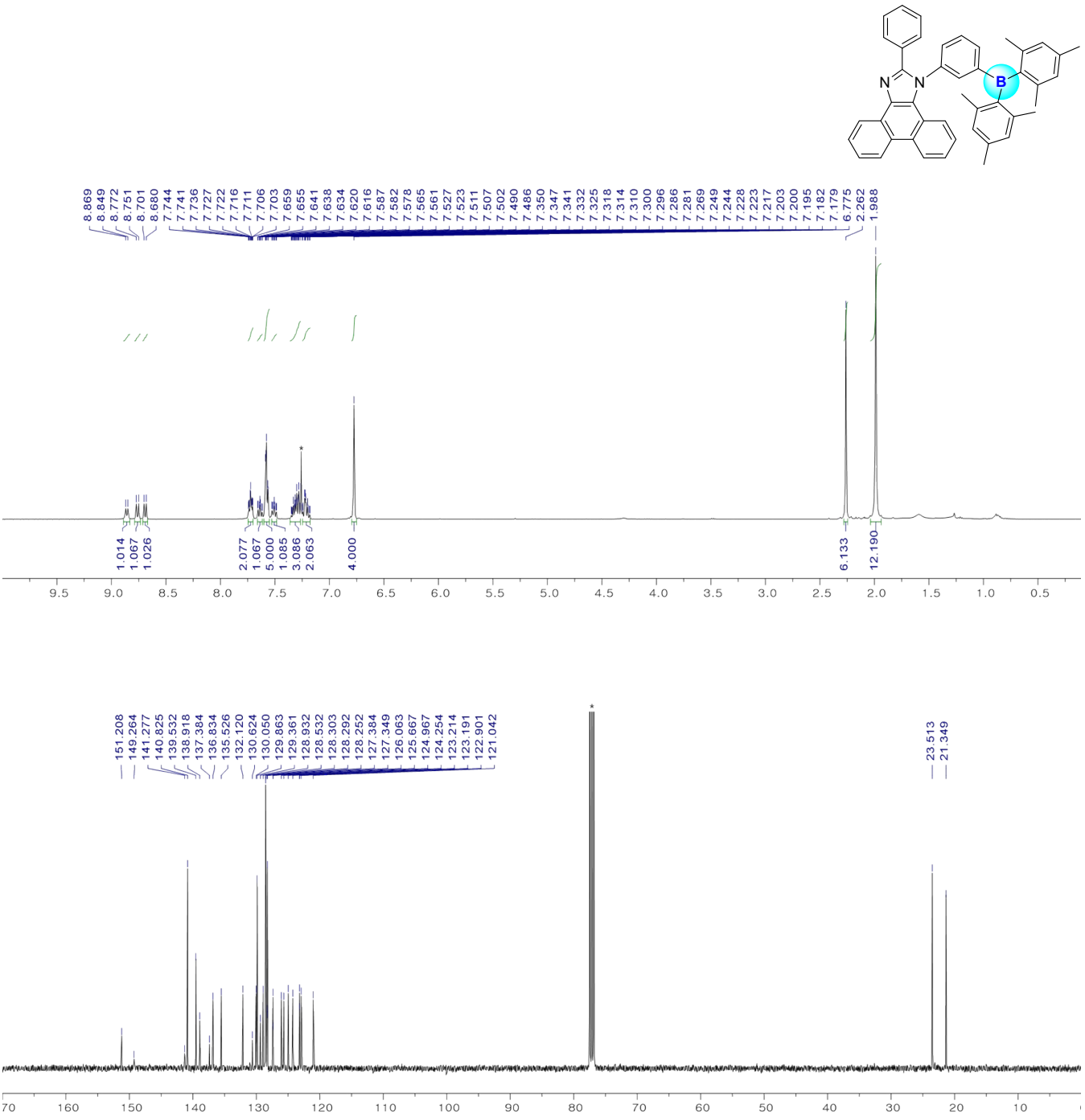

Fig. S24 ^{1}H (top) and ^{13}C (bottom) NMR spectrum of **2Ph** (∗ from residual $CHCl_3$ in $CDCl_3$).

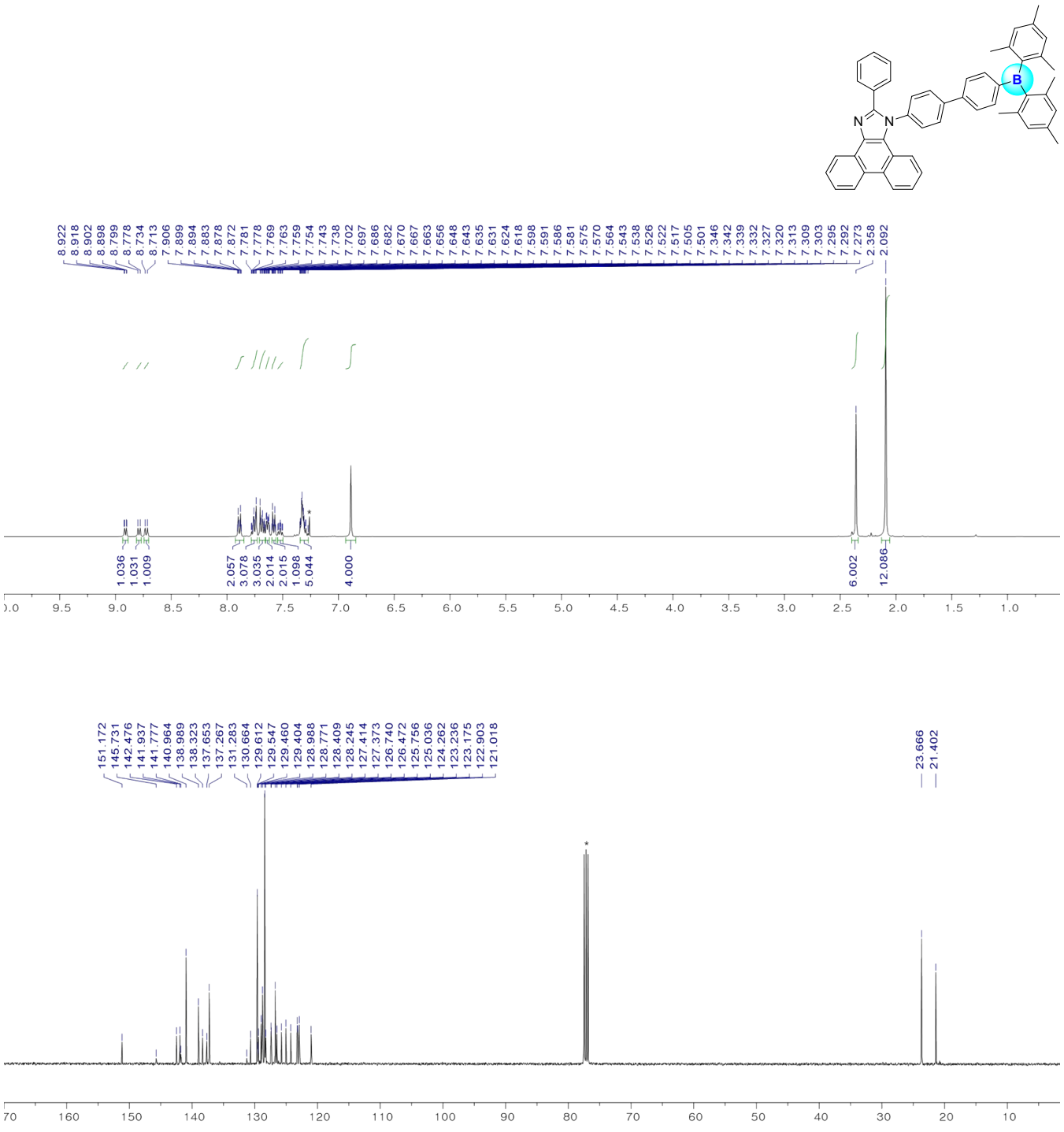

Fig. S25 ^{1}H (top) and ^{13}C (bottom) NMR spectrum of **1BP** (∗ from residual $CHCl_3$ in $CDCl_3$).

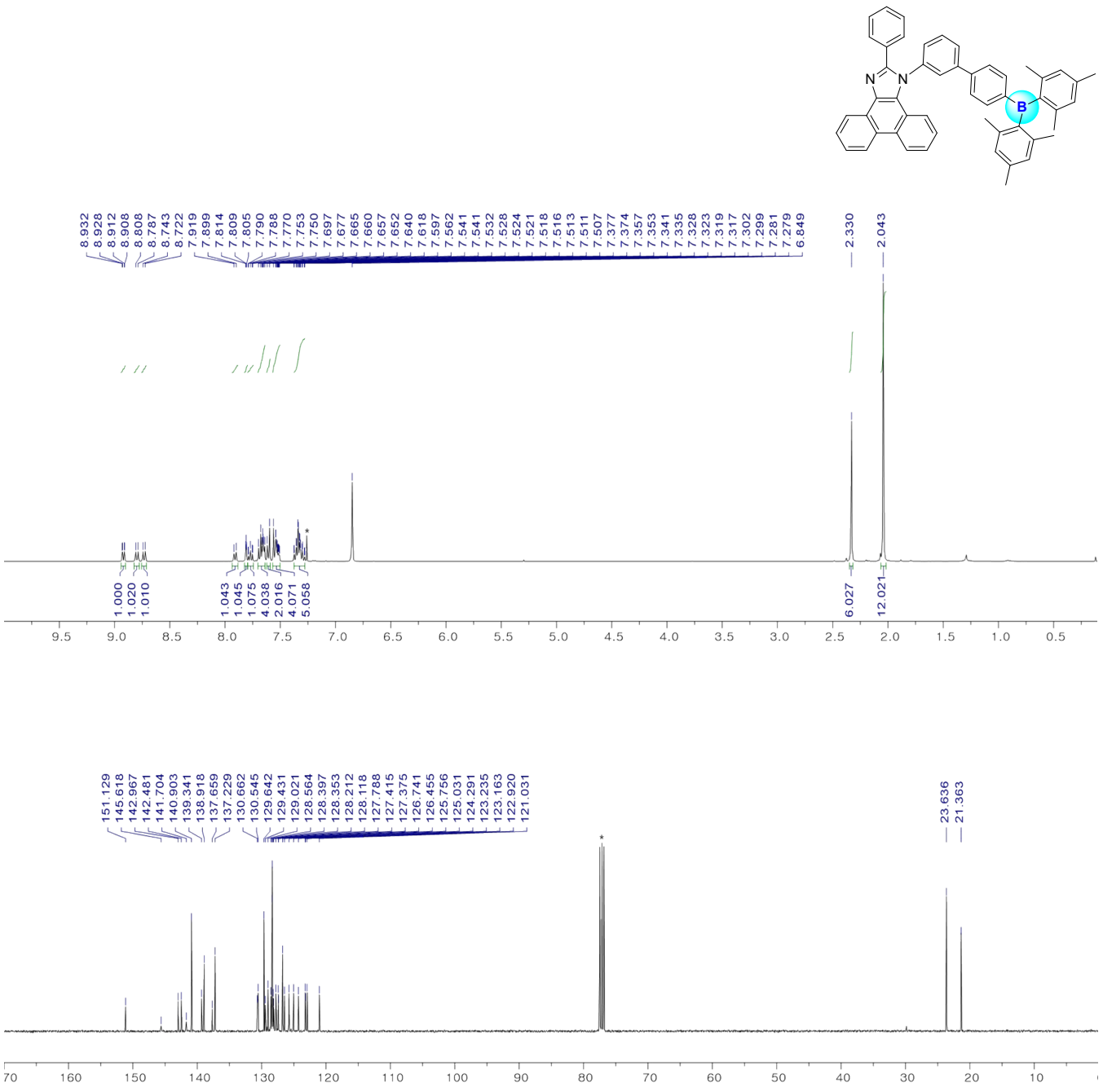

Fig. S26 ^{1}H (top) and ^{13}C (bottom) NMR spectrum of **2BP** (∗from residual $CHCl_3$ in $CDCl_3$).